Ionian Sea circulation as clarified by assimilation of glider observations

Srdjan Dobricic[1]

Centro Euro-Mediterraneo per i Cambiamenti Climatici, Bologna, Italy

Nadia Pinardi

Corso di Scienze Ambientali, Università di Bologna

and

Istituto Nazionale di Geofisica e Vulcanologia, Bologna, Italy

Pierre Testor

LOCEAN-IPSL, Paris, France,

Uwe Send

SIO, La Jolla, CA, USA

Corresponding author: Srdjan Dobricic, CMCC, Viale Aldo Moro 44, Bologna, Italy, e-mail: dobricic@bo.ingv.it

Abstract

Glider observations of temperature and salinity in the Ionian Sea (Eastern Mediterranean Sea), made in the period October 2004-December 2004, were assimilated into an operational forecasting model together with other in-situ and satellite observations. The impact of glider data on the estimation of the circulation is studied and it is found that the assimilation of glider data significantly improve the vertical structure of temperature and salinity fields and remove biases. The accurate representation of the dynamical structures due to the assimilation of glider data allowed a detailed analysis of the dynamics of the Atlantic Ionian Stream (AIS). During autumn and in the Sicily Strait, the AIS is strengthened by the positive but weak wind stress curl near the southern Sicilian coast and by the temperature gradient between the warm surface mixed layer and the cold upwelled waters near Sicily. In winter the change of position of the wind stress curl zero line and the cooling of the surface mixed layer forces the AIS to shift southward in the Ionian Sea. The AIS is shown for the first time to pinch off an eddy in the Ionian Sea.

1. Introduction

The Mediterranean Forecasting System (MFS) (Pinardi *et al*. 2003) provides daily analyses of the circulation of the Mediterranean Sea. The analyses are based on the production of background fields by a high resolution general circulation model and the assimilation of in-situ and satellite data using a multivariate assimilation scheme. One of the major challenges of MFS is to assimilate the largest possible number of satellite and in-situ observations in real time. The multivariate assimilation scheme currently assimilates at the same time satellite Sea Level Anomalies (SLA) and Sea Surface Temperature (SST) and in-situ observations of temperature and salinity profiles by eXpendable BathyThermographs (XBT) and Argo floats. However, the assimilation of observations from additional types of instruments has the potential to provide an improvement in the quality and accuracy of MFS analyses. New observing systems are required for an efficient monitoring of the basin scale structures, and MFS started to investigate the importance of gliders that measure temperature and salinity in the top 200m of the ocean.

The analyses offer the opportunity to study in detail the dynamics of interesting circulation structures because they produce best estimates of circulation fields based on observations that are dynamically consistent in space and time. In particular, glider measurements, which can be repeated for several months in the same area, could greatly improve estimates of the thermal, salinity and circulation structures at least in the measurement area. The glider used here surveyed the central-western Ionian Sea, an area characterized by an intense surface circulation called the Atlantic Ionian Stream (AIS) (Robinson *et al*. 1999). The AIS is one of the branches of the Modified Atlantic Water (MAW) stream system that enters the Sicily Strait and occupies the central-northern part of the Strait, near the southern coasts of Sicily (Fig. 1). At the Maltese escarpment, the AIS detaches from the continental shelf and slope region of the Sicily Strait and enters the 3000m

deep Ionian basin. Historical in-situ and satellite observations and modeling studies indicate complex circulation patterns of the AIS at the entrance to the Ionian Sea and a high interannual variability (e.g. Malanotte-Rizzoli 1997, Robinson *et al*. 1999, Lermusiaux and Robinson 2001, Pinardi *et al*. 2006). The most detailed investigation of the physical structure and properties of the AIS circulation was obtained with detailed "Conductivity-Temperature-Depth" (CTD) surveys between 1994 and 1996 and by the assimilation of observations into a regional oceanographic model (Robinson *et al*. 1999, Lermusiaux and Robinson 2001). In the modeling study by Demirov and Pinardi (2002) the AIS interannual variability is induced by changes of the wind stress curl in the Ionian Sea. On the other hand, the modeling study by Napolitano *et al*. (2003), found that the internal dynamics and interaction of the flow with the complex topography in the Sicily Strait have a major impact on the seasonal variability of the AIS. Furthermore, Pierini and Rubino (2001) and Molcard *et al*. (2002a) find in their modeling studies that even in the absence of wind stress forcing, density gradients between MAW and the Levantine Intermediate Water (LIW) are sufficient to create realistic circulation patterns of the AIS. The modeling study by Sorgente *et al*. (2003) confirms that the density gradients have a major impact on the meandering of the AIS. A general picture that emerges from modeling studies is that the AIS undergoes large hydrodynamic instabilities due to its vertical density structure, and on the interannual scale its path is influenced by the atmospheric wind stress curl. However, the relative importance of each forcing component on shorter temporal scales has not been completely investigated.

During its repeated passes in the western Ionian Sea, the glider crossed a meander of the AIS and provided information about the initial development and subsequent detachment of an anticyclonic eddy from the AIS. The aim of this study is to show that by assimilating high-resolution glider data together with other in-situ and satellite observations it is possible to obtain an optimal data set which can then be used to study the time variability of the AIS

and the underlying dynamical mechanisms. Furthermore, the study will show the methodology for future operational assimilation of glider observations in the Mediterranean Sea and estimate its relative impact on the local quality of the MFS analyses.

The paper is organized as follows: Section 2 will describe the methodology. It will give an overview of the glider observations, describe the Mediterranean general circulation model and the data assimilation scheme. Section 3 will compare the control analyses with the analyses which assimilated glider observations. It will show the impact of the glider observations on the quality of the MFS analyses in the Ionian Sea. Section 4 will describe the major mechanisms which control the temporal variability of the surface circulation of the AIS in the Strait of Sicily and the Ionian Sea. Conclusions will be offered in Section 5.

2. Data and methods

2.1 Glider observations

Gliders are autonomous underwater vehicles of a small size that can 'fly' underwater along slightly inclined paths by changing their density. The buoyancy force results in forward velocity (~40cm/s) as well as vertical motion (~15cm/s). So gliders move on a sawtooth pattern, gliding downwards when denser than the surrounding water and upwards when buoyant. The high efficiency of the propulsion system enables them to be operated for several months. They can be steered remotely and the measurements can be downloaded during surfacing by a two-way communication system via satellite. When at surface, gliders also take Global Positioning System (GPS) fixes to correct the dead reckoning positions used for navigation. This gives an estimate of the horizontal currents averaged over the glider trajectory between two contact GPS fixes.

In the period 1 October 2004 - 2 December 2004 a glider (Davis *et al*. 2003) from the Webb Research Corporation was deployed in the Ionian Sea. The glider made observations of conductivity, temperature, and pressure along a section which spanned ~300km to the south east of the Italian coast (Fig. 2). It was programmed to dive to 200 m depth and collected 4254 downcasts in about 3 months of operations at a rate of approximately 50 profiles per day; the distance between profiles being approximately 500 m. It had contact with land every eight profiles (~4 hours). Classical CTD profiles carried out during the deployment/recovery operations at a few hundred meters from the first/last glider profile allowed the calibration of the conductivity cell in order to match an accuracy of 0.005 in salinity.

2.2 Mediterranean model set-up

The Mediterranean Sea model set-up (Tonani et al., 2008) is based on the free surface version of the OPA 8.2 model (Roullet and Madec 2000). Its horizontal resolution is $1/16^{o}$, and the domain spans from 18^{0}W to 36^{0}E and 30^{0}N to 46^{0}N. The model covers the whole Mediterranean Sea and includes a part of the Atlantic Ocean. At the boundaries in the Atlantic, temperature and salinity fields are relaxed towards the Levitus climatology (Levitus *et al*. 1998), and the cross-boundary fluxes are set to zero. The model has 72 levels defined in the vertical. The top level is 3 m thick, and the resolution gradually decreases toward the bottom layers. Horizontal diffusion and viscosity are defined by a bi-Laplacian operator with the constant diffusion coefficient $K_H=5x10^9 m^4 s^1$ and viscosity coefficient $K_M=3x10^9 m^4 s^{-1}$. The vertical diffusion is parameterized in terms of the mixing scheme developed by Pacanowski and Philander (1981), with the addition of enhanced constant vertical value of the mixing coefficient in case of vertical instabilities. The advection of tracers uses a second order accurate upstream scheme (Webb *et al*. 1998), whilst the momentum advection uses an energy conservative form of the central differencing scheme. Surface fluxes are calculated interactively every 6 hours (Castellari *et al*. 1998) using operational analyses of air temperature, humidity, winds and cloud cover from the European Centre for Medium-range Weather Forecasts (ECMWF). A detailed description of the model set-up is given in Tonani *et al*. (2008). The model simulation initial condition is set to correspond to January 1, 2002 using the temperature and salinity MEDATLAS climatology (The MEDAR Group 2002).

2.3 Data assimilation scheme

The data assimilation scheme is based on the previous implementation of the Reduced Order Optimal Interpolation (ROOI) scheme in the Mediterranean (De Mey and Benkiran 2002; Demirov *et al*. 2003, Dobricic *et al*. 2005). It assimilates satellite sea level anomaly, in-situ temperature and salinity profiles with a multivariate error background matrix, producing updates in model sea level, salinity, temperature and velocity fields. Surface heat fluxes are corrected by a term proportional to the difference between the temperature at the top model layer and objective analyses of the satellite sea surface temperature. The coefficient of the relaxation applied in the surface heat fluxes correction is 40 $Wm^{-2} K^{-1}$.

Horizontal and vertical modes of the background error covariance matrix are assumed to be independent. The horizontal background error correlations are assumed to be Gaussian and a function of the distance only using an horizontal correlation radius of 23 km. This value is estimated empirically from the evaluation of the horizontal correlation of misfits between background fields and SLA observations in the period 2001-2004. As the Rossby radius of deformation in the Mediterranean is about 10-15 km (e.g. Robinson *et al*. 1987) the corresponding typical length scale of eddies is 50-100km (Stammer 1997, Eden 2007) and the used correlation scale is smaller than the average eddy size.

Multivariate Emprirical Orthogonal Functions (EOFs) estimated from sea level, temperature, salinity and barotropic stream function covariances are used to represent the background error correlations in the vertical direction. The Mediterranean Sea is divided into 13 regions with different physical properties, and EOFs are calculated in each region and for each season from the variability around the mean of a model run spanning the time period 1993-2000. All the details of this assimilation scheme are found in Dobricic *et al*. (2005) and Dobricic *et al*. (2007).

The analyses are produced starting from 1 January 2003 with a weekly assimilation cycle until June 2004 and once a day with a daily assimilation cycle thereafter. The assimilation of SLA observations uses the mean dynamic topography calculated by Rio *et al*. (2006), based on a model estimate (Demirov *et al*. 2003) and observations by surface drifters in the period 1993-1997.

3. Assimilation of glider observations

The temporal and spatial frequency of glider observations is far too high for the adapted assimilation scheme which assumes geostrophic balance between density and sea level corrections and an assimilation window of one day. Furthermore, given the assumed horizontal error correlation scale of 23km, observations spaced ~500m would not be independent. It is then customary to average observations within a space-time influence radius before they are assimilated (e.g. Daley 1991). The raw observations were averaged within a daily time window, giving rise to observations spaced approximately 25 km. This spacing is represented by approximately four model grid points at 1/16 degrees model resolution. Corrections at shorter space scales could be seen as 2-delta-x noise and easily removed during the model integration. Hereafter we refer to 'control' analyses as the product of an assimilation run without glider data. This section will compare control analyses to the analyses which assimilated glider observations, so-called glider assimilation analyses.

Fig. 3 shows a Hovmoller diagram of the daily averaged glider observations for temperature. In autumn 2004, the vertical stratification changed from a shallow thermocline in

October (around 30m deep) to a weaker and deeper thermocline in November, and to a well mixed ocean in December. The control analyses were capable to reproduce the high vertical stratification in October, the deepening of the mixed layer in November and the enhanced vertical mixing in December, but did not depict some of the mesoscale features that were observed by the glider, and the thermocline was not sharp enough. For example, the glider observations show the deepening of isotherms, probably corresponding to anticyclonic motion, on October 10 and 30, November 8 and December 1, whereas the control analyses show only a weak signal. On the other hand, the glider assimilation analyses show these mesoscale features and have a smaller cold temperature bias below the thermocline.

Daily averaged observations of salinity are shown in Fig. 4. The observed minima of salinity, corresponding to the core of MAW, show the position of the AIS in agreement with previous observations (e.g. Lermusiaux and Robinson 2001). In October the salinity minimum is located at the depth of ~40m. Its position becomes deeper in November, and reaches ~60m on 1 December. Furthermore, in November the salinity minimum extends from the ocean surface to the depth of ~50m, indicating enhanced vertical mixing. Fig. 4 shows also that the control analyses are in general capable to depict the major path of the AIS but they estimate a weaker salinity minimum at the depth of ~50m. during the period 28 October-10 November. The assimilation of glider observations corrects the salinity field (Fig. 4) in the proper direction and produces a marked minimum of the salinity at ~50m. It also increases the salinity in layers deeper than ~100m, thus reducing the low salinity bias of the control analyses.

Fig. 5 shows estimates of the average horizontal velocity in the top 200m of the ocean obtained by the glider, control and glider assimilation analyses. Velocity observations by the glider were not assimilated and therefore represent an independent data set for the validation. Only the first and last glider track crossing of the Ionian Sea are shown (see Fig. 2). The

major circulation features along the trajectory of the glider are quite accurately estimated by the control analyses. In fact, the control analyses show that there is an anticyclonic meander of the AIS, and a cyclonic circulation between the Sicilian coast and the AIS. The major difference between observations and the control analyses is in the intensity of the velocity field, with the control analyses showing weaker transports. The assimilation of temperature and salinity observations by the glider improves the velocity estimates by generally increasing the intensity of the velocity field. On the other hand, at smaller scales along the track, the assimilation of glider observations does not always improve the velocity estimates. For example, in November 2004 around 36.2N, the control analyses are in better agreement with glider observations than glider assimilation analyses. This could be due to the averaging of glider observations that produces unrealistic assimilation corrections and a related unrealistic dynamical adjustment by the model. It should be noted that the assimilation of glider velocity observations would further increase the accuracy of the analyses (e.g. Taillandier *et al*. 2006). The assimilation of velocity observations by gliders will be possible in the future by applying a new three-dimensional variational scheme developed for the same forecasting model (Dobricic and Pinardi 2007).

In order to further assess how glider observations impact surface circulation estimates, Fig. 6 shows daily snapshots of the difference in surface elevation between the glider assimilation and the control analyses during and after the observational period. As expected, during the assimilation of glider observations (October-November) the surface elevation differences are localized close to the glider path. In the next two months (December and January) the differences remain along the path of the AIS in the Ionian Sea, but they extend also in the southern Levantine especially around 26^0E. Here the AIS detaches from the African coast and forms the western flank of the Mersa Matruh gyre (Pinardi *et al.*, 2006). The rapid spreading of differences in sea surface elevation along the AIS in January indicates

that there was a remote interaction between the circulation in the Ionian Sea and the Levantine basin. In the latter, the AIS branches and forms different currents, among them the Mid-Mediterranean and the southern Levantine jet (e.g. Pinardi *et al*. 2006). By assuming that the lower boundary of the main thermocline is at approximately 300m and that the reduced gravity is 6.75×10^{-3} m s^{-2}, Molcard *et al*. (2002b) estimated that Kelvin waves complete the eastern basin circumvolution in about 7 months. Using this estimate we can explain the differences in sea surface elevation found in the Levantine, one month after the end of the glider experiment and the assimilation of observations. In the bottom right panel in Fig. 6 the sea level differences are larger around the Mersa Matruh border than westward of this point. In this area the differences may be amplified due to non-linear instabilities of the free current forming the border of the gyre, and may reach the same amplitude as near the observations area in the Ionian Sea.

4. Analysis of surface circulation in the Ionian Sea

This section discusses the structure of the surface circulation in the Ionian Sea and Sicily Strait during and after the glider assimilation period, as estimated by the glider assimilation analyses.

Fig. 7 shows that at the end of October there is a strong AIS current in the middle of the Sicily Strait crossing the region between Malta and the Sicilian coast. The AIS enters the Ionian Sea as a strong jet forming a well-defined meander with first a cyclonic and then an anticyclonic curvature. At the end of November, the cyclonic circulation north-westward of the meander, enlarges becoming a western boundary intensified cyclonic gyre. This gyre has been depicted many times in model simulations. It has been schematized by Pinardi *et al*.

(2006) and called the Western Ionian cyclonic gyre (Fig. 1). At the end of December, the AIS weakens in the Sicily Strait, going closer to the southern Sicily coastlines. The Western Ionian anticyclonic gyre (Fig.1) becomes stronger and retroflects the meander. In the following months, the AIS is still strong in the Ionian Sea, whilst it weakens in the Sicily Strait. In January-February, the Western Ionian anticyclonic gyre changes and in March the northernmost part of the meander detaches an anticyclonic eddy.

In order to obtain further insight into the dynamical processes that determine the surface circulation changes between autumn and winter, the surface dynamic height is calculated with respect to 400m (Fig. 8). The reference level of 400 m allowed to estimate the dynamic height even in the Sicily Strait. On the other hand, this reference depth may cut across the LIW layer, and the assumptions of no motion will not be valid anymore. Therefore, surface dynamic height maps were calculated with deeper reference levels, but qualitatively the results did not change. Furthermore, comparing Fig. 7 and Fig. 8, we note the similarity between sea surface height and surface dynamic height, thus confirming that we can work with this reference level assumption. These results are also in agreement with findings by Malanotte-Rizzoli *et al*. (1997), who estimated that in the Sicily Strait and the western part of the Ionian Sea the surface dynamic height is mainly determined by buoyancy gradients in the top 250m of the water column.

In Fig. 8 the surface dynamic height is also calculated using either only temperature or salinity fields in order to estimate their separate influence on the surface circulation. This subdivision shows that in autumn temperature and salinity contribute with a similar intensity to the dynamic height along the path of the AIS. Furthermore, in the Sicily Strait (12.5^0E,36.5^0N) and in the area where AIS enters the Ionian Sea (17^0E,35.5^0N) temperature gradients contribute more to the strength of the AIS than salinity gradients. In the Sicily Channel, horizontal temperature gradients are formed in summer, because the local conditions

produce upwelling that induces a strengthening of the eastward flowing AIS current along the southern coast of Sicily. The upwelling along the southern coast of Sicily occurs regularly each summer and is discussed in several studies (e.g. Moretti *et al*. 1993, Robinson *et al*. 1999, Marullo *et al*. 1999, Lermusiaux and Robinson 2001). It is mainly influenced by the wind stress, inertia of the isopycnal domes and topographic effects (Lermusiaux and Robinson 2001). The border of the area with upwelled cold waters defines the position of the surface AIS in the Sicily Strait and the horizontal temperature gradients due to the upwelling enhance the AIS. Thus in autumn the temperature and salinity contribution to the dynamic height are of the same importance. At the end of winter (March) the temperature-derived dynamic height is negligible and the salinity-derived surface dynamic height gradients prevail in determining the position and intensity of the AIS. The upper layer mixing during winter weakens the horizontal temperature gradients while salinity structures, such as MAW salinity minima, come to the surface and directly influence the surface circulation (e.g. Molcard *et al*. 2002a).

Another process that may influence the surface circulation is the wind stress curl. In fact, the AIS during the end of summer/beginning of autumn period flows very close to the zero line of the wind stress curl in the Sicily Strait, as seen from Fig.9. The zero line separates two different wind vorticity areas, one cyclonic along the coast of Sicily and the other anticyclonic in the southern regions. After leaving the Sicily Strait and entering the Ionian Sea, the AIS becomes a free open ocean jet. However, even there the AIS flows approximately along the zero wind stress curl line. The positive curl to the north of the AIS in the Ionian forces the Western Ionian cyclonic Gyre that forms in autumn and continues to develop during winter. South of the AIS however, the curl is weak and does give rise only to the recurrent Western Ionian anticyclonic Gyre which is unstable and extremely variable in amplitude and position. The persistent forcing by the wind stress positive curl in September-

October along the southern and eastern coasts of Sicily enhances the upwelling in the Sicily Strait and the open ocean Ekman pumping in the eastern Sicily side.

The comparison between the curl in autumn and in winter (Fig. 9) shows that the major difference is in the strength and extension of the curl positive area, due to the seasonal changes in wind intensity and structure. This difference in the wind forcing is partially responsible for the different dynamics of the AIS between autumn and winter. During winter the positive curl area widens and the zero curl line shifts to the south of Malta. The AIS bifurcates then around Malta (located at 36^0N and 14.5^0E) with one branch remaining close to the southern coast of Sicily, and the other flowing south of Malta. Comparison of Fig. 7 with Fig. 9 shows that the second branch is approximately located along the wind stress curl zero line in winter. The Western Ionian anticyclonic Gyre, trapped inside the area of the positive curl in winter, is weakened by the increased Ekman pumping as well as the large non-linear anticyclonic meander seen in January in Fig. 6. This effect could be partially responsible for the small anticyclonic eddy detachment from the AIS (Fig. 7).

We conclude then that the position of the curl zero line and the intensity of the winter wind stress curl significantly influence the path of the AIS in the Sicily Strait and the Ionian Sea. This finding confirms the results of the modeling experiments by Demirov and Pinardi (2002), in which the positive curl over the whole northern Ionian Sea in winters 1981-1987 induced a large cyclonic circulation in the northern Ionian Sea, whilst the negative curl in the northern Ionian Sea in winters 1988-1993 induced a well defined and persistent Western Ionian anticyclonic Gyre and anticyclonic meander of the AIS. Our study further indicates that the structure and intensity of the summer curl around Sicily may also influence the extension and intensity of the AIS in the Sicily Strait and the quantity of the MAW advected in the northern Ionian Sea. The MAW in the northern Ionian Sea remains trapped in winter in the positive curl area and possibly reduce the impact of the positive curl on the circulation.

Our analyses are also in agreement with modeling results presented in Pierini and Rubino (2001), Molcard *et al*. (2002a) and Napolitano *et al*. (2003) in which the model simulations are performed without the wind stress forcing. In that case, in analogy with our weak wind forcing case of the autumn period, the AIS would flow naturally to the north along the southern Sicilian shelf like it it is shown by Napolitano *et al*. (2003), where the strong upwelling centers south of Sicily were present in the initial condition.

5. Conclusions

We have shown that the assimilation of temperature and salinity observations from gliders in the Ionian Sea improved the Mediterranean Forecasting System (MFS) basin scale analyses. It removed cold and fresh biases below the mixed layer and helped to represent the Modified Atlantic Water (MAW) subsurface maxima along the Atlantic Ionian Stream (AIS) path. The differences in the surface circulation due to the assimilation of glider observations in comparison to the control analyses were on small spatial scales, indicating that the control analyses were already depicting the regional-scale surface circulation with a relatively high accuracy. After the period of direct observations, the impact of assimilation was persisting, but also moving away from the glider area. In the months following glider observations, assimilation of glider data impacted the southern Levantine basin, indicating a coupling process between the Ionian and the southern Levantine area through the AIS.

The quality of the analyses during the glider assimilation period gives confidence in looking at the dynamical evolution of the AIS. The analyses show that between autumn and winter the AIS shifted southward and pinch off an anticyclonic eddy. During autumn the AIS

forms a well defined meander between the Western Ionian cyclonic and Western Ionian anticyclonic Gyres. The meander relaxed during winter and the Western Ionian anticyclonic gyre weakened.

Two major processes force the seasonal variability of AIS path and dynamics. The first process is related to the positive wind stress curl area extension, the position of the zero curl line and the second to the large-scale cooling of the mixed layer in winter and the weakening of horizontal temperature gradients. As a consequence, the AIS has two distinguishable regimes of flow. The first appears in autumn (and probably summer) when the temperature gradients enhances the AIS intensity in the Sicily Strait, whilst the positive Ekman pumping is weak and concentrated close to the Sicily coasts. The second is in winter when the horizontal temperature gradients and the intensity of the AIS weakens in the Sicily Strait, whereas the positive Ekman pumping region strengthens and extends south of Malta. The Western Ionian anticyclonic gyre weakens by the enlarged Ekman pumping area and the AIS shifts position southward, close to the wind stress curl zero line. Almost at the end of winter, an anticyclonic eddy detached from the northern tip of the AIS probably due to the combination of all these forcing and the AIS instabilities.

In addition to providing a new insight into the processes that govern the surface circulation in the Sicily Strait and the Ionian Sea, the study shows that the glider observations improved the quality of the basin scale analyses. Several new deep ocean gliders are being deployed in the Mediterranean. They are capable to measure temperature and salinity profiles down to 1000 m and it is fair to expect that they will significantly improve the quality of the basin scale analyses in the Mediterranean.

Acknowledgements

This work was partially funded by EU projects MFSTEP (Mediterranean Forecasting System: Towards Environmental Predictions, Contract number: EVK3-CT-2002-00075) and MERSEA (Marine Environment and Security for the European Area, Contract number: SIP3-CT-2003-502885). Special thanks to Giuseppe Zappalà of the Istituto Talassografico of Messina who helped with the logistics of the glider experiment.

References

Castellari, S., Pinardi, N., and K. D. Leaman, 1998: A model study of air-sea interactions in the Mediterranean Sea. *J. Mar. Sys.*, **18**, 89-114.

Daley, R., 1991: Atmospheric data analysis. *Cambridge University Press*, 457 pp.

Davis, R. E., Eriksen, C. E., and C. P. Jones, 2003: Autonomous buoyancy-driven underwater gliders, *in Technology and applications of autonomous underwater vehicles, G. Griffiths Ed., Taylor and Francis*, 37-58.

De Mey, P., and M. Benkiran, 2002: A multivariate reduced-order optimal interpolation method and its application to the Mediterranean basin-scale circulation. *Ocean Forecasting, Eds. Pinardi N. and J. Woods, Springer Verlag*, 281-306.

Demirov, E., and N. Pinardi, 2002: Simulation of the Mediterranean Sea circulation from 1979 to 1993. Part I: The interannual variability. *J. Mar. Sys.*, **33-34**, 23-50.

Demirov, E., Pinardi, N., Fratianni, C., Tonani, M., Giacomelli, L. and P. De Mey, 2003: Assimilation scheme in the Mediterranean forecasting system: operational implementation. *Annales Geophysicae*, **21**, 189-204.

Dobricic, S., Pinardi, N., Adani, M., Bonazzi, A., Fratianni, C., and M. Tonani, 2005: Mediterranean Forecasting System: An improved assimilation scheme for sea-level anomaly and its validation. *Q. J. R.. Meteor. Soc*., **131**, 3627-3642.

Dobricic, S., Pinardi, N., Adani, M., Tonani, M., Fratianni, C., Bonazzi, A., and V. Fernandez, 2007: Daily oceanographic analyses by Mediterranean Forecasting System at the basin scale. *Ocean Sciences*, **3**, 149-157.

Dobricic, S., and N. Pinardi, 2008: An oceanographic three-dimensional variational data assimilation scheme. *Ocean Modell.*, in press.

Eden, C., 2007: Eddy length scales in the North Atlantic Ocean. *J. Geophys. Res.*, **112**, doi:10.1029/2006JC003901.

Lermusiaux, P. F. J., and A. R. Robinson, 2001: Features of dominant mesoscale variability, circulation patterns and dynamics in the Strait of Sicily. *Deep Sea Res.*, **48**, 1953-1997.

Levitus S., Boyer T.P., Conkright M.E., O'Brien T., Antonov J., Stephens C., Stathoplos L., Johnson D. and R. Gelfeld, 1998: NOAA Atlas NESDIS 18, World Ocean Database 1998, U.S. Gov. Printing Office, Wash., D.C., 346pp + set of Cd-roms.

Malanotte-Rizzoli, P., Manca, B. B., Ribera D'Alcala, M., Theocharis, A., Bergamasco, A., Bregant, D., Budillon, G., Civitarese, G., Georgopoulos, D., Michelato, A., Sansone, E., Scarazzato, P., and E. Souvermezoglou, 1997: A synthesis of the Ionian Sea hydrography, circulation and water mass pathways during POEM-Phase I, *Prog. Oceanog.*, **39**, 153-204.

The MEDAR Group, 2002: MEDAR/MEDATLAS 1998-2001 Mediterranean and Black Sea database of temperature, salinity and bio-chemical parameters and climatological atlas (4 CDRoms), *Internet server* *www.ifremer.fr/sismer/program/medarIFREM*ER/TMSI/IDM/SISMER Ed., Centre de Brest

Molcard, A., Gervasio, L., Griffa, A., Gasparini, G. P., Mortier, L., and T.M. Özgökmen, 2002a: Numerical investigation of the Sicily Channel dynamics: density currents and water mass advection. *J. Mar. Sys.*, **36**, 219-238.

Molcard, A, Pinardi, N., Iskandarani, M., and D. B. Maidvogel, 2002b: Wind driver general circulation of the Mediterranean Sea simulated with a spectral element ocean model. *Dyn. Atmos. Ocean.*, **35**, 97-130.

Moretti, M., Sansone, E., Spezie, G., and A. De Maio, 1993: Results of investigations in the Sicily Channel (1986-1990). *Deep-Sea Res.*, **40**, 181-1192.

Napolitano E., Sannino, G., Artale, V., and S. Marullo, 2003: Modeling the baroclinic circulation in the area of the Sicily channel: The role of stratification and energy diagnostics, *J. Geophys. Res.*, **108**, 3230, doi:10.1029/2002JC001502

Pacanowski, R. C., and S. G. H. Philander, 1981: Parameterization of vertical mixing in numerical models of tropical oceans, *J. Phys. Oceanogr*., **11**, 1443-1451.

Pierini, S., and A. Rubino, 2001: Modeling the oceanic circulation in the area of the Strait of Sicily: The remotely forced dynamics, *J. Phys. Oceanogr.*, **31**, 1397–1412.

Pinardi, N., Allen, I., Demirov, E., De Mey, P., Korres, G., Lascaratos, A., Le Traon, P.-Y., Maillard, C., Manzella, G., and C. Tziavos, 2003: The Mediterranean ocean forecasting system: first phase of implementation (1998-2001). *Annales Geophysicae*, **21**, 3-20.

Pinardi, N., Arneri, E., Crise, A., Ravaioli M., and M. Zavatarelli**,** 2006**:** The physical, sedimentary and ecological structure and variability of shelf areas in the Mediterranean Sea**.** *The Sea* Vol. 14 (A. R. Robinson and K. Brink Eds.), Harvard University Press, Cambridge, USA, 1243-1330.

Robinson, A. R., Hecht, A., Pinardi, N., Bishop, J., Leslie, W. G., Rosentroub, Z., Mariano, A. J., and S. Brenner, 1987: Small synoptic/mesoscale eddies and energetic variability of the eastern Levantine basin. *Nature*, **327**, 131-134.

Robinson, A. R., Sellschopp, J., Warn-Varnas, A., Leslie, W. G., Lozano, C. J., Haley Jr., P. J, Anderson, L. A., and P. F. J. Lermusiaux, 1999: The Atlantic Ionian Stream. *J. Mar. Sys.*, **20**, 129-156.

Roullet, G., and G. Madec, 2000: Salt conservation, free surface and varying volume: a new formulation for ocean GCMs. *J. Geophys. Res.*, **105**, 23927-23942.

Sorgente, R., Drago, A. F., and A. Ribotti, 2003: Seasonal variability in the Central Mediterranean Sea circulation. Ann. Geophys., **21**, 299–322.

Stammet, D., 1997: Global characteristics of ocean variability estimated from regional TOPEX/POSEIDON altimeter measurements. *J. Phys. Ocean.*, **27**, 1743-1769.

Taillandier, V., Griffa, A., and A. Molcard, 2006: A variational approach for the reconstruction of regional scale Eulerian velocity fields from Lagrangian data. *Ocean Modelling*, **13**, 1-24.

Tonani, M., Pinardi, N., Dobricic, S., Adani, M., and F. Marzocchi, 2008: A high resolution free surface general circulation model of the Mediterranean Sea. *Ocean Sciences*, **4**, 1-14.

Webb, D.J., deCuevas, B.A., and C.S. Richmond: 1998: Improved advection schemes for ocean models. *J. of Atm. and Ocean. Tech.*, **15**, 1171--1187.

List of figures:

Figure 1: Bottom topography of the Sicily Strait and the Ionian Sea (m), and path of major surface currents drawn after Pinardi *et al*. (2006). The dotted line shows the path of the glider in the period October 2004-December 2004. Circulation features indexed by numbers are: 1 – Western Ionian cyclonic Gyre, 2 – Western Ionian anticyclonic Gyre and 3 - African MAW Current.

Figure 2: The path of the glider in the period 1 October 2004-23 December 2004. Dots indicate the daily averaged positions of the glider. The bottom topography is also displayed. Isobaths are 250m, 500m, 1000m, 2000m and 3000m.

Figure 3: Daily averaged vertical temperature profiles (^{0}C) along the path of the glider for the period October-December 2004. Upper panel: glider observations, averaged daily; Middle panel: control daily analyses. Lower panel: glider assimilation analyses.

Figure 4: Same as Fig. 3, but for salinity.

Figure 5: Estimates of the horizontal velocity averaged between 0 and 200m depth (ms^{-1}) along the glider track: glider observations (left panels), control analysis (central panels) and analyses with glider observations (right panels). Top panels show estimates in the period 1 October 2004-13 October 2004, at the beginning of the observational period. Bottom panels show estimates from 13 November 2004 till 2 December 2004, at the end of the observational period.

Figure 6: Differences between daily averaged sea surface elevation of glider assimilation and control analyses. The contour interval is 2cm, and the zero line is not plotted. Solid lines show positive and dashed lines negative values. The time is indicated at the right corner of each picture.

Figure 7: Daily averaged surface elevation (cm) for six days between October 31, 2004 and March 31, 2005. Arrows indicates the position in the Ionian Sea of the anticyclonic meander of the AIS, located between the Western Ionian anticyclonic and cyclonic Gyres, and the anticyclonic eddy detached from the AIS.

Figure 8: Surface dynamic height (cm) with respect to a 400m reference level on 31 October 2004 (left panels) and 31 March 2005 (right panels). Top panels show the surface dynamic height calculated using both temperature an salinity profiles, middle panels show the dynamic height calculated using only temperature, and bottom panels using only salinity. Blank ocean areas are shallower than 400 m.

Figure 9: Mean wind stress (Nm^{-2}) and its curl ($10^{-6}Nm^{-3}$) in the period September-October 2004 (top panel) and February-March 2005 (bottom panel). The positive wind curl is shaded grey.

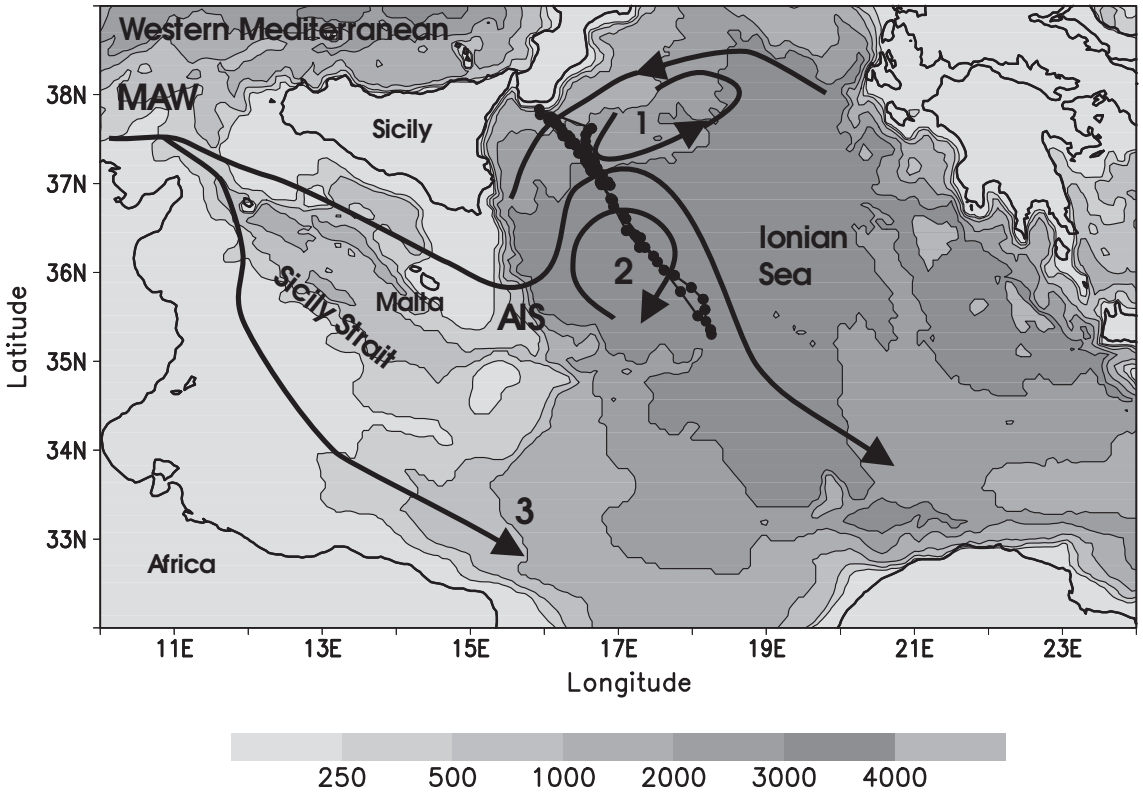

Figure 1: Bottom topography of the Sicily Strait and the Ionian Sea (m), and path of major surface currents drawn after Pinardi *et al*. (2006). The dotted line shows the path of the glider in the period October 2004-December 2004. Circulation features indexed by numbers are: 1 – Western Ionian cyclonic Gyre, 2 – Western Ionian anticyclonic Gyre and 3 - African MAW Current.

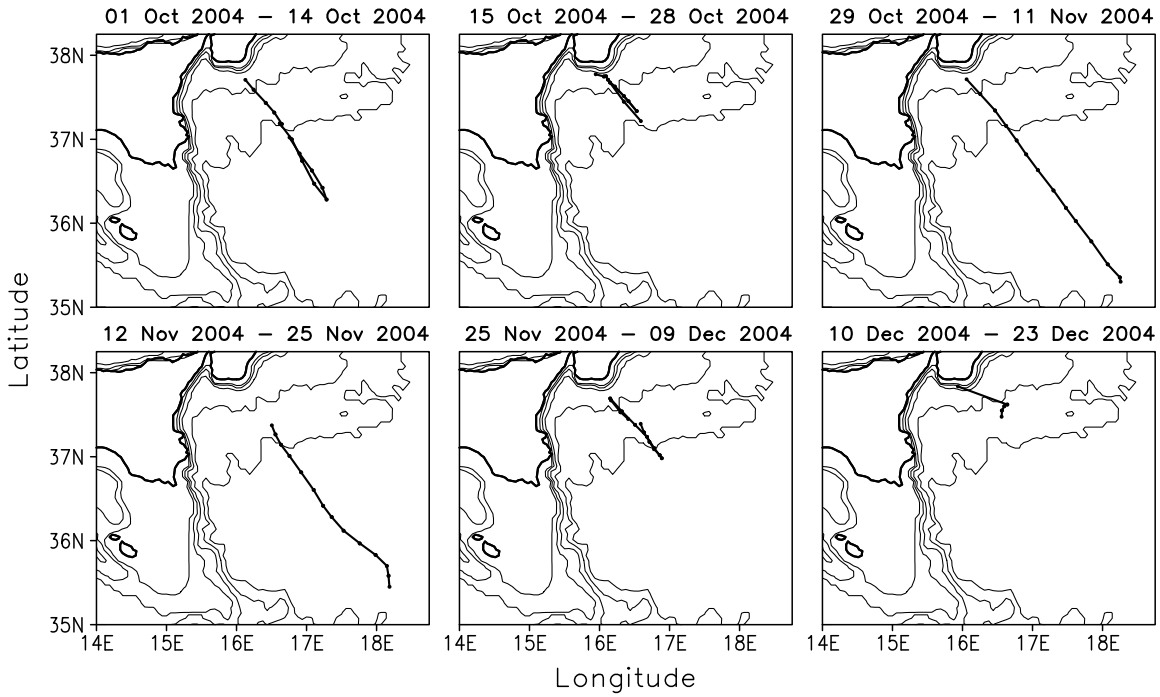

Figure 2: The path of the glider in the period 1 October 2004-23 December 2004. Dots indicate the daily averaged positions of the glider. The bottom topography is also displayed. Isobaths are 250m, 500m, 1000m, 2000m and 3000m.

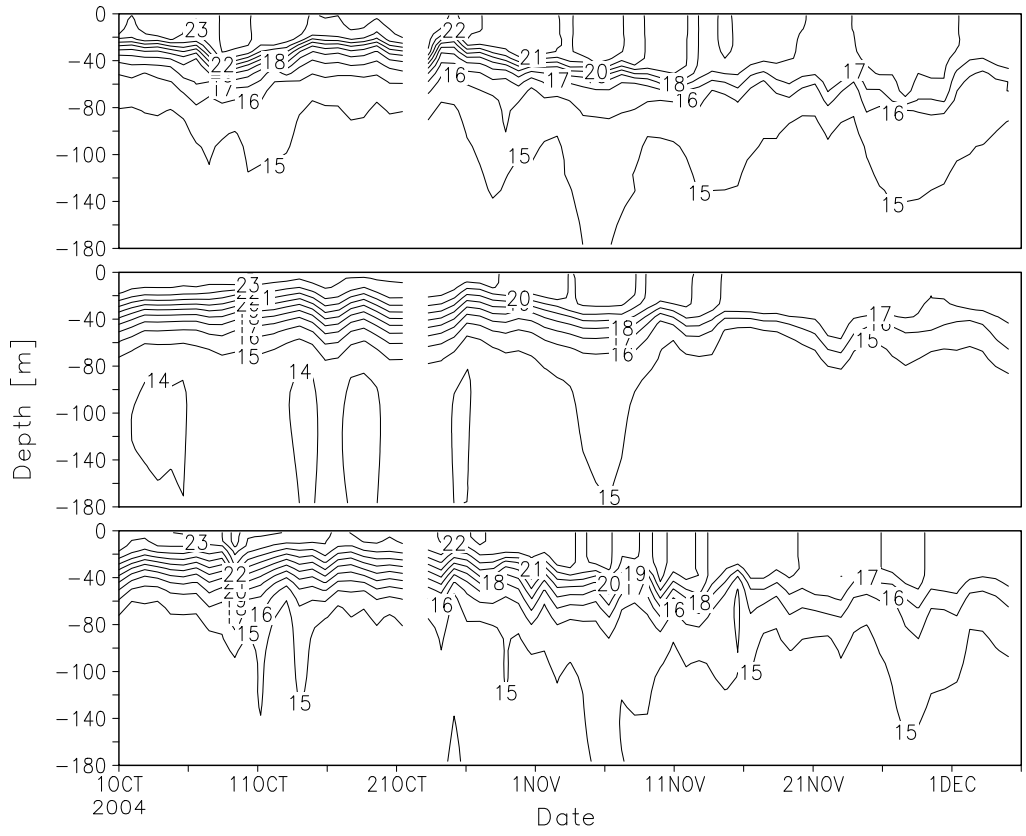

Figure 3: Daily averaged vertical temperature profiles (^{0}C) along the path of the glider for the period October-December 2004. Upper panel: glider observations, averaged daily; Middle panel: control daily analyses. Lower panel: glider assimilation analyses.

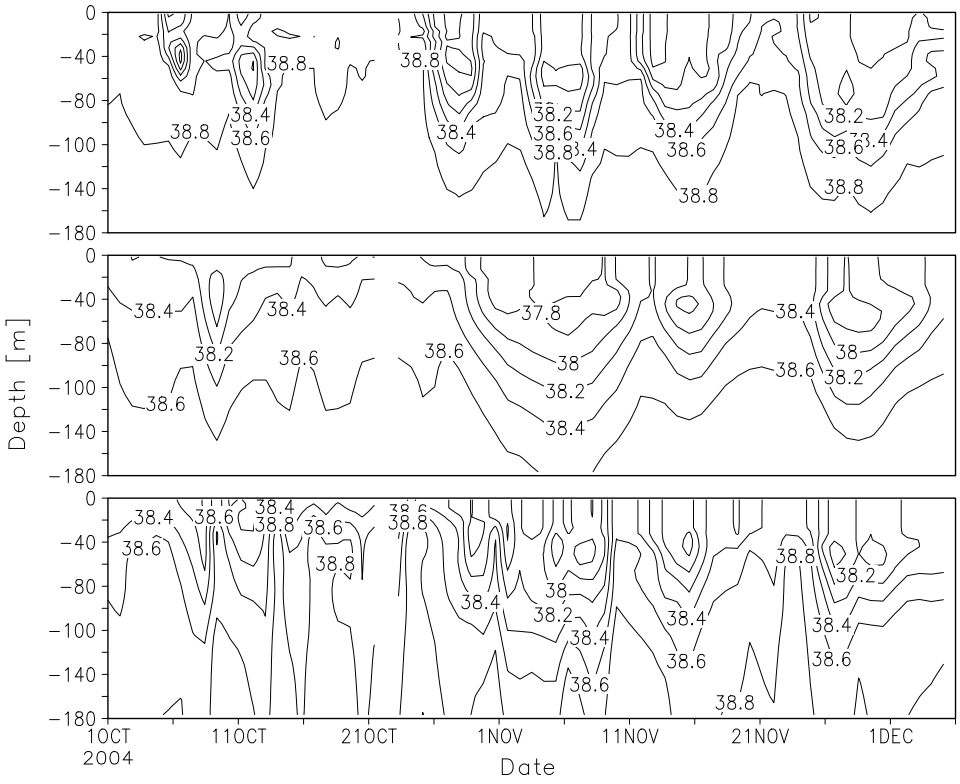

Figure 4: Same as Fig. 3, but for salinity.

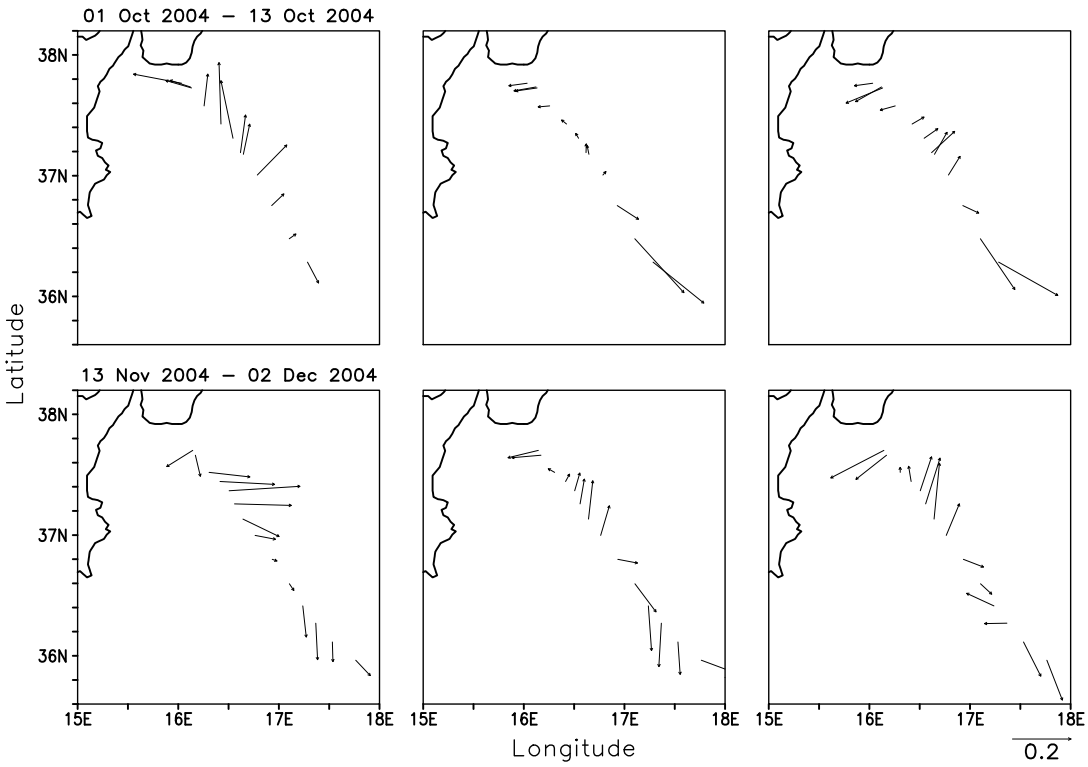

Figure 5: Estimates of the horizontal velocity averaged between 0 and 200m depth (ms^{-1}) along the glider track: glider observations (left panels), control analysis (central panels) and analyses with glider observations (right panels). Top panels show estimates in the period 1 October 2004-13 October 2004, at the beginning of the observational period. Bottom panels show estimates from 13 November 2004 till 2 December 2004, at the end of the observational period.

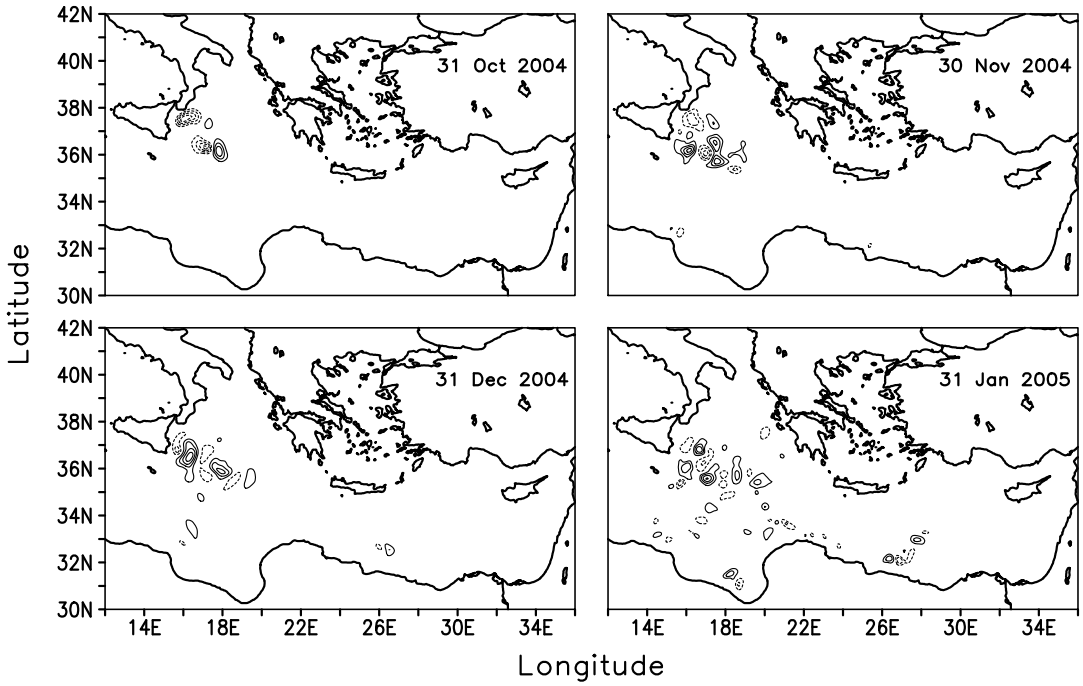

Figure 6: Differences between daily averaged sea surface elevation of glider assimilation and control analyses. The contour interval is 2cm, and the zero line is not plotted. Solid lines show positive and dashed lines negative values. The time is indicated at the right corner of each picture.

Figure 7: Daily averaged surface elevation (cm) for six days between October 31, 2004 and March 31, 2005. Arrows indicates the position in the Ionian Sea of the anticyclonic meander of the AIS, located between the Western Ionian anticyclonic and cyclonic Gyres, and the anticyclonic eddy detached from the AIS.

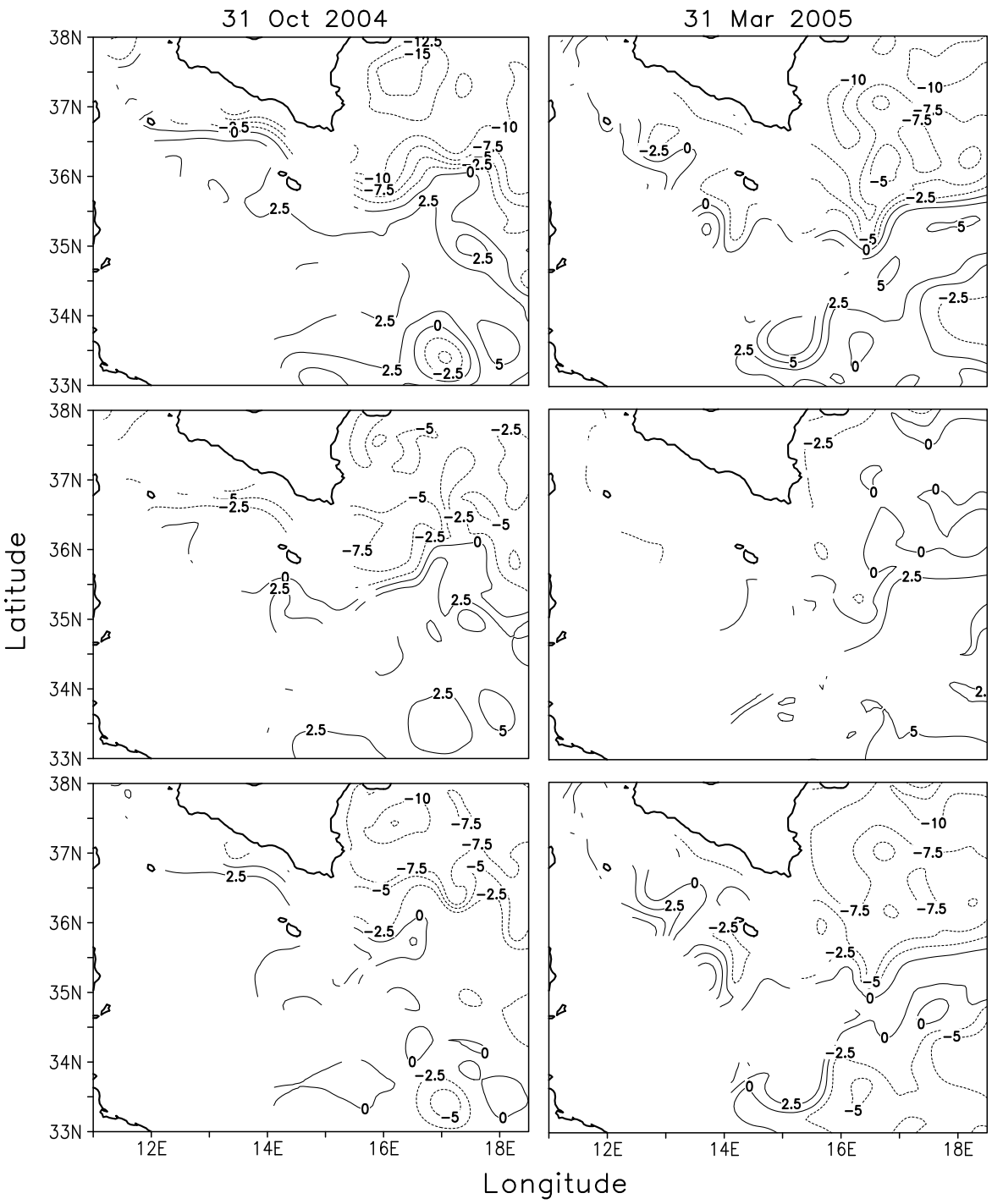

Figure 8: Surface dynamic height (cm) with respect to a 400m reference level on 31 October 2004 (left panels) and 31 March 2005 (right panels). Top panels show the surface dynamic height calculated using both temperature an salinity profiles, middle panels show the dynamic height calculated using only temperature, and bottom panels using only salinity. Blank ocean areas are shallower than 400 m.

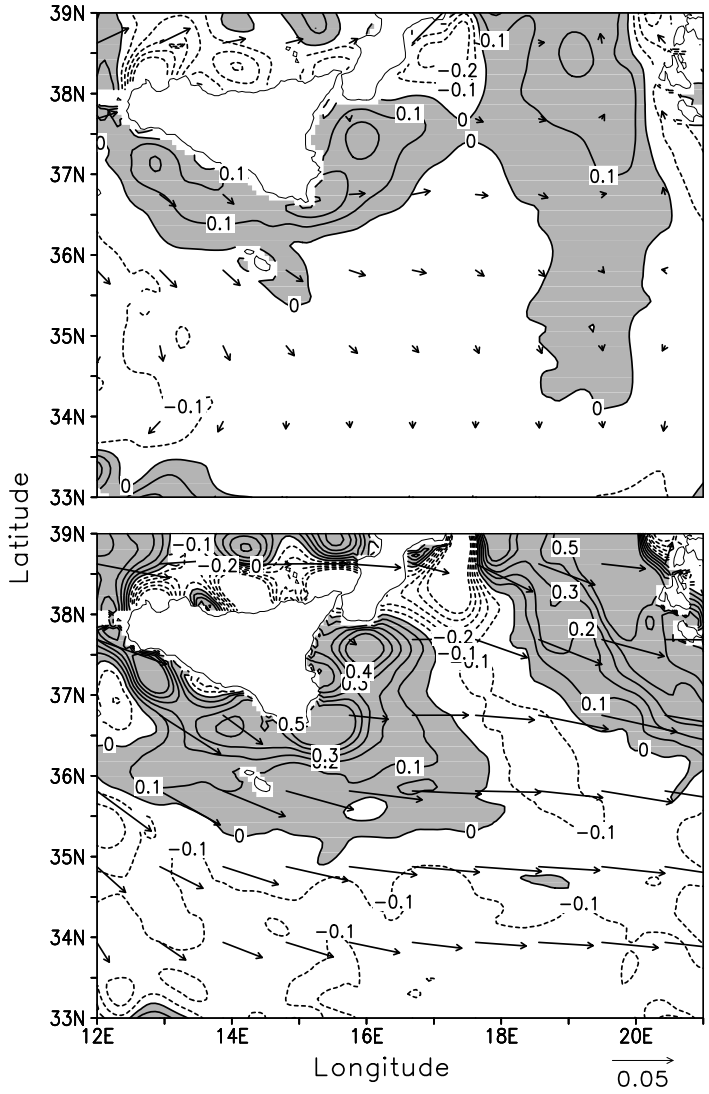

Figure 9: Mean wind stress (Nm^{-2}) and its curl ($10^{-6}Nm^{-3}$) in the period September-October 2004 (top panel) and February-March 2005 (bottom panel). The positive wind curl is shaded grey.